Input Functions for 6-[Fluorine-18]Fluorodopa Quantitation in Parkinsonism: Comparative Studies and Clinical Correlations

Shugo Takikawa, Vijay Dhawan, Thomas Chaly, William Robeson, Robert Dahl, Italo Zanzi, Francine Mandel, Phoebe Spetsieris and David Eidelberg

Departments of Neurology, Research, Medicine and Biostatistics, North Shore University Hospital/Cornell University Medical College, Manhasset, New York

PET has been used to quantify striatal 6-[^{18}F]fluoro-L-dopa (FDOPA) uptake as a measure of presynaptic dopaminergic function. Striatal FDOPA uptake rate constants (K_i) can be calculated using dynamic PET imaging with measurements of the plasma FDOPA input function determined either directly or by several estimation procedures. **Methods:** We assessed the comparative clinical utility of these methods by calculating the striato-occipital ratio (SOR) and striatal K_i values in 12 patients with mild to moderate PD and 12 age-matched normal volunteers. The plasma FDOPA time-activity curve (K_i^{FD}); the plasma ^{18}F time-activity curve (K_i^{F}); the occipital time-activity curve (K_i^{OCC}); and a simplified population-derived FDOPA input function (K_i^{EFD}) were used to calculate striatal K_i. **Results:** Mean values for all striatal K_i estimates and SOR were significantly lower in the PD group. Although all measured parameters discriminated PD patients from normals, K_i^{FD} and K_i^{EFD} provided the best between-group separation. K_i^{FD}, K_i^{EFD} and K_i^{OCC} measures correlated significantly with quantitative disease severity ratings, although K_i^{FD} predicted quantitative clinical disability most accurately. **Conclusion:** These results suggest that K_i^{FD} may be an optimal marker of the parkinsonian disease process. K_i^{EFD} may be a useful alternative to K_i^{FD} for most clinical research applications.

Key Words: PET; 6-[^{18}F]fluoro-L-dopa; input function; multiple time graphical approach; Parkinson's disease; discriminant analysis; nigrostriatal dopaminergic function

J Nucl Med 1994; 35:955–963

Quantitative PET has been used with 6-[^{18}F]fluoro-L-dopa (FDOPA) as a means of assessing presynaptic nigrostriatal dopaminergic function in life. FDOPA/PET techniques have been employed to provide an objective measure of disease severity in Parkinson's disease (PD) patients, as well as to identify individuals with early or preclinical involvement (*1,2*). These applications have importance in assessing the effects of neuroprotective therapies and fetal transplantation on disease progression (*3*), and in identifying individuals at risk on a genetic or environmental basis. However, to be useful for these purposes, FDOPA/PET must yield quantitative parameters that: (1) Correlate closely with independent disease severity measures; and (2) Discriminate reliably between patients with mild early disease, or with preclinical involvement, and normal control subjects.

A variety of analytical methods have been developed to quantitate FDOPA/PET images for these purposes. Simple target-to-background calculations from the striatum and occipital regions have provided useful information without blood sampling (*4,5*). Subsequently, the multiple time graphical approach (MTGA) (*6,7*) has been developed to estimate kinetic rate constants for striatal FDOPA uptake (K_i's) based upon the time courses of striatal and plasma FDOPA radioactivity (*8,9*). These calculations require extensive arterial blood sampling and high-performance liquid chromatographic (HPLC) analysis of plasma samples to determine the precise input function for FDOPA. Alternatively, investigators have employed the plasma ^{18}F time-activity curve (TAC) without HPLC metabolite correction (*10,11*), and the occipital time-activity curve without blood sampling (*2,11–14*). Both these methods assume a fixed decreasing relationship between FDOPA and its major metabolite 3-O-methyl-FDOPA (3-OMFD) in plasma throughout the course of the FDOPA/PET study (*15,16*).

In spite of the theoretical and technical advantages to each of these techniques (*16*), little is known about their comparative merits as discriminators of early disease and as predictors of clinical severity. To address this issue, we studied 12 mild-moderate PD patients and 12 normal control subjects with FDOPA/PET and examined the clinical correlates of the parameters estimated according to each of the various methodological approaches.

MATERIALS AND METHODS

Subjects

The following subject groups were studied with quantitative FDOPA/PET:

Received Jul. 19, 1993; revision accepted Oct. 26, 1993.

For correspondence or reprints contact: Dr. David Eidelberg, Dept. of Neurology, North Shore University Hospital/Cornell University Medical College, 300 Community Dr., Manhasset, New York 11030.

TABLE 1
Clinical Summary: Parkinson's Disease Patients

Patients	Age	Sex	HY	Tremor	Rigidity	Akinesia	Gait	Motor*
1	38	M	II	++	−	++	−	12
2	27	F	III	++	++	++	++	27
3	32	M	III	−	++	++	+	17
4	84	M	III	+++	++	++	++	32
5	42	F	II	+	+	+	−	12
6	38	M	II	+	++	++	−	12
7	77	M	I	++	+	+	−	9
8	69	F	I	+	++	++	−	12
9	66	F	III	++	++	+	++	21
10	67	M	III	+	+	+	+	18
11	54	M	I	+	+	++	−	7
12	69	F	III	++	++	++	++	23

*Motor scores refer to the Unified Parkinson Disease Rating Scale (UPDRS) composite scores (UPDRS 3.0; items 19–31).
HY = Hoehn and Yahr Stage.

Normal Subjects. We studied 12 normal volunteer subjects (9 men and 3 women; mean age ±s.d., 51 ± 18 yr) recruited by an advertisement among the hospital personnel of North Shore University Hospital/Cornell University Medical College and the spouses of PD patients in local support groups. The following exclusion criteria were used: (1) past history of neurological or psychiatric illness; (2) prior exposure to neuroleptic agents or drug use; (3) past medical history of hypertension, cardiovascular disease and diabetes mellitus; and (4) abnormal neurological examination.

Patients with Parkinson's Disease. We studied 12 classical PD patients without dementia (7 men and 5 women; age 52 ± 19 yr). A diagnosis of PD was made if the patient had "pure" parkinsonism without a history of known causative factors such as encephalitis or neuroleptic treatment; did not have early dementia, supranuclear gaze palsy, or ataxia; and had a convincing response to levodopa. In all patients family history was negative for neurodegenerative illnesses. This group was selected with mild to moderate clinical involvement [Hoehn and Yahr Stages I–III (*17*); see Table 1].

Ethical permission for these studies was obtained from the Institutional Review Board of North Shore University Hospital/Cornell University Medical College. Written consent for all subjects was obtained following a detailed explanation of the scanning procedure.

Positron Emission Tomography

All patients and normal volunteers fasted overnight prior to PET scanning. All antiparkinsonian medications were discontinued at least 12 hr before PET investigations. At the time of the PET study, all PD patients were rated quantitatively according to the Hoehn and Yahr Scale and the Unified Parkinson Disease Rating Scale (UPDRS 3.0) (*18*). PET studies were performed using the Super PETT 3000 tomograph (Scanditronix, Essex, MA). The performance characteristics of this instrument have been described elsewhere (*19*). This four-ring BaF_2 time-of-flight whole-body tomograph acquires 14 PET slices with z-axis gantry translation of one half-ring distance every 30 sec. Each slice is 8 mm thick and reconstructed with an in-plane resolution of 7.5 mm FWHM in the high-resolution mode.

Subjects were positioned in the scanner in a custom molded headrest [Alpha Cradle, Smithers Medical, Tallmadge, Ohio (*20*)] with three-dimensional laser alignment. The gantry angle of the tomograph was adjusted to be parallel to the orbitomeatal line. A cylindrical tube filled with ^{68}Ge was placed in the field of view to provide real-time calibration for each slice. All studies were performed with eyes open in a dimly lit room and minimal auditory stimulation. FDOPA was produced according to the radiochemical synthesis of Luxen (*21*) and was >95% radiochemically pure (specific activity approximately 400 mCi/mmole). All subjects received 200 mg carbidopa 1 hr before the study to inhibit decarboxylation. FDOPA (5–10 mCi) in 20–40 ml saline was injected into an antecubital vein over 45 sec with an automated infusion pump. The transit time from injection point to the brain (brain delay) was measured by the coincidence counter on the scanner. Emission scanning began simultaneously with the start of the FDOPA injection, and continuous scan data were acquired in the list mode between 0 and 100 min postinjection. PET images were reconstructed with a correction for tissue attenuation of 511 keV and gamma radiation measured with external ^{68}Ge sector source. PET reconstructions were also corrected for random coincidences, electronic dead time and scatter effects.

The time course of plasma ^{18}F radioactivity was determined by radial arterial blood sampling followed by plasma centrifugation. Sixteen 9-sec samples were taken by a precision peristaltic pump followed by nine discrete samples taken at 3.5, 5, 10, 25, 40, 55, 70, 85 and 100 min postinjection. Plasma ^{18}F radioactivity in each sample was represented as a ratio of its activity divided by ^{68}Ge activity in a calibration tube. Because the first 16 arterial samples were collected using a pump, an appropriate smearing correction was applied (*22*). In the six blood samples taken at 10, 25, 40, 55, 70 and 85 min postinjection, plasma FDOPA was separated from its metabolites using HPLC with radiochemical detection. The details of the HPLC analysis were described elsewhere (*15*).

Image Analysis

Region of interest (ROI) analysis was performed on 256 × 256 PET reconstructions using a SUN microcomputer (490 SPARC Server) and Scan/VP Software (*23*). Striatal and occipital ROIs were identified by visual inspection with reference to a standard neuroanatomical atlas (*24*). Elliptical ROIs were placed interactively on composite (40–100 min) PET brain slices to outline the whole striatum (mean 90 pixels/striatum; pixel size 4 mm^2). Irregular occipital ROIs (16–20 cm^2) were defined on the first 10-min scan (0–10 min) to avoid sampling activity in the transverse sinuses and torcula. Occipital count rates were assumed to represent background activity referrable to nonspecific FDOPA uptake in extrastriatal tissues and untrapped metabolites. Occipital activity concentrations were subtracted from striatal ^{18}F-activity concentrations measured in each of six 10-min scans acquired between 40 and 100 min postinjection to obtain the time profile for specific striatal activity for FDOPA, i.e., counts referrable to trapped FDOPA, ^{18}F-fluorodopamine and its metabolites. Count rates in striatal and occipital ROIs were normalized by activity in the real-time calibration source measured in each PET slice.

Kinetic measures of FDOPA uptake were calculated by MTGA (*6,7*) using the time course of striatal radioactivity from 40 to 100 min postinjection and each of the following four input functions.

Plasma FDOPA Time-Activity Curve. The input function for plasma FDOPA was determined using arterial blood sampling and HPLC analysis as described above. The time course of specific (background subtracted) striatal FDOPA concentration divided by plasma FDOPA activity was plotted against the ratio of the

TABLE 2
FDOPA Fractions at Each Sampling Time Postinjection

		10 min	25 min	40 min	55 min	70 min	85 min
Normal (n = 12)	mean (s.d.)	0.71 (0.06)	0.49 (0.06)	0.38 (0.05)	0.31 (0.04)	0.26 (0.04)	0.23 (0.04)
PD (n = 12)	mean (s.d.)	0.68 (0.07)	0.46 (0.06)	0.34 (0.05)	0.28 (0.04)	0.24 (0.03)	0.21 (0.03)
Total (n = 24)	mean (s.d.)	0.70 (0.06)	0.48 (0.06)	0.36 (0.05)	0.29 (0.04)	0.25 (0.04)	0.22 (0.04)
	COV	9.2%	12.1%	13.5%	13.6%	13.9%	16.3%

PD = Parkinson's disease; s.d. = standard deviation; and COV = coefficient of variation defined as (s.d. mean) × 100 (%).

plasma FDOPA time-integral-to-the plasma FDOPA concentration. In the MTGA, the slope of this line represents the rate constant of FDOPA uptake into the striatum (*8,9,15*). Striatal K_i values calculated in this way were designated K_i^{FD}.

Estimated Plasma FDOPA Time-Activity Curve. The plasma FDOPA time-activity curve was estimated using a population-based ^{18}F time-activity curve with a standardized metabolite correction derived through the analysis of plasma HPLC data obtained from 10 subjects not included in this study. This technique requires only minimal blood sampling and no HPLC. The computational details and validation of this estimation procedure are presented in the Appendix. For individual subjects, the population-based ^{18}F time-activity curve was scaled by two arterial samples at 10 and 40 min postinjection. A metabolite correction was then applied based upon the population-based FDOPA breakdown curve to produce an estimate of the individual FDOPA time-activity curve. Striatal K_i values calculated by the MTGA using this estimated input function were designated K_i^{EFD}.

Plasma ^{18}F Time-Activity Curve. The time course of the total plasma ^{18}F activity without an HPLC metabolite correction was used as an input function for the MTGA. The time course of striatal ^{18}F activity (background not subtracted) (*11*) divided by plasma ^{18}F concentration was plotted against the ratio of the plasma ^{18}F time-integral-to-plasma ^{18}F concentration (*10,11*). Striatal K_i values calculated in this way were designated K_i^P.

Occipital ^{18}F Time-Activity Curve. As an alternative noninvasive approach, the time course of occipital ^{18}F activity was used as an input function (*12,13*). In this analysis, we determined the occipital ^{18}F time-activity curve in serial 10-min PET images acquired over a full 100 min beginning at the time of injection. The time course of striatal/occipital activity was plotted against the ratio of integrated occipital-to-occipital activity to obtain striatal K_i values, designated as K_i^{OCC} which was expressed as min^{-1} and K_i^{FD}, K_i^{EFD} and K_i^P were expressed as ml/min/g. In all patient and control scans, we additionally calculated the ratio of striatal-to-occipital activity (SOR) by dividing striatal count rates by occipital count rate measured on the last 10-min scan (90–100 min postinjection).

Statistical Analysis

The statistical procedures were performed using SAS (SAS Institute; Cary, NC). (1) Mean striatal K_i^{FD}, K_i^{EFD}, K_i^P and K_i^{OCC} values and SOR for the PD group were compared with analogous control values using a paired Student's t-test. (2) Between-group discrimination for each of the parameters was assessed using a stepwise procedure with the F-test associated with Wilk's λ (*25*). In this analysis, left and right striatal measures for the PD patients were considered independently and compared with mean right and left striatal values measured for the normal volunteers. Within subjects, left and right striatal K_i^{FD}, K_i^{EFD}, K_i^P, K_i^{OCC} and SOR measures were significantly correlated in the normal control group ($r > 0.6$; $p < 0.03$), but were uncorrelated in the PD patient group ($r < 0.5$; $p > 0.1$). (3) In the PD group, we correlated mean striatal K_i and SOR values with Hoehn and Yahr scores and with UPDRS composite motor scores (UPDRS 3.0; items 19–31; (*18*)] by computing Pearson product-moment correlation coefficients. (4) We correlated K_i^{EFD}, K_i^P, K_i^{OCC} and SOR with K_i^{FD} for all subjects using Pearson product-moment correlation coefficients.

RESULTS

Plasma Analysis

Table 2 shows mean FDOPA fractions (±s.d.) in total plasma radioactivity at six sampling points (10, 25, 40, 55, 70 and 85 min postinjection) in the normal and PD groups. In the 24 subjects, FDOPA fractions did not vary greatly across individuals, with coefficients of variation (COV = s.d./mean) at each time point <20%. Mean FDOPA fractions in the PD patients were somewhat lower than those in the normal controls. However, these differences were not significant at each time point. Additionally, no statistical difference in the rate of change of the FDOPA fraction between pairs of consecutive time points (repeated measures analysis of variance, $p > 0.1$) was evident between the PD and normal groups. These findings suggest that peripheral FDOPA breakdown is similar in the control and patient groups.

FDOPA/PET Analysis

Mean values of SOR, K_i^{FD}, K_i^{EFD}, K_i^P and K_i^{OCC} are given in Table 3. As expected from the inclusion of FDOPA metabolites in the plasma, ^{18}F and occipital time-activity curves, K_i^P and K_i^{OCC} were numerically lower than K_i^{FD} and K_i^{EFD} in which a metabolite correction was performed. In normals, the intersubject variability of the various parameters differed, with K_i^{OCC} having the greatest variability (COV = 27.1%). By contrast, COV was smallest for SOR (9.4%). In the PD group, mean values of each parameter were significantly lower than corresponding normal control values ($p < 0.001$). Mean K_i values for the PD group showed similar reductions in magnitude relative to normal values (44%–52% of the normal levels); mean SOR was 75% of the normal control mean.

Discriminant analysis indicated that K_i^{FD} and K_i^{EFD} distinguished PD patients from normals more accurately than the other parameters, although all K_i discriminants were

TABLE 3
Striatal Ki's for the Four Input Functions and Striato-to-Occipital Ratio

		SOR	K_i^{P*}	K_i^{OCC*}	K_i^{FD*}	K_i^{EFD*}
Normal (n = 12)	Mean	2.11	0.0070	0.0066	0.0129	0.0127
	s.d.	0.20	0.0011	0.0018	0.0023	0.0024
	COV	9.6%	15.5%	27.1%	17.8%	18.8%
PD (n = 12)	Mean	1.58	0.0031	0.0034	0.0062	0.0059
	s.d.	0.15	0.0013	0.0014	0.0015	0.0015
	COV	9.4%	39.8%	40.0%	24.2%	25.1%

*See text for definitions of K_i^P, K_i^{OCC}, K_i^{FD} and K_i^{EFD}. K_i^{OCC} is expressed as min^{-1}; the other parameters are expressed as ml/min/g.

PD = Parkinson's Disease; COV = coefficient of variation defined as (s.d./mean) × 100 (%); and SOR = striato-to-occipital ratio.

highly significant (F[1, 34] = 120.4, 117.9, 87.6, and 34.9 for K_i^{FD}, K_i^{EFD}, K_i^P, and K_i^{OCC}, respectively; $p < 0.0001$, Fig. 1). Striatal K_i^{FD} and K_i^{EFD} correctly classified all normals and PD patients. SOR discriminated PD patients from normals less accurately than K_i^{FD} and K_i^{EFD} (F[1, 34] = 86.4), although better than K_i^{OCC}.

In the PD group, correlation analysis revealed a significant negative relationship between Hoehn and Yahr scores and striatal K_i^{FD} ($r = -0.68$, $p < 0.02$), K_i^{EFD} ($r = -0.63$, $p < 0.03$) and K_i^{OCC} ($r = -0.61$, $p < 0.04$), but not between these scores and K_i^P or SOR. UPDRS composite scores correlated significantly only with striatal K_i^{FD} ($r = -0.60$, $p < 0.04$; Fig. 2), but not with K_i^{EFD}, K_i^P, K_i^{OCC} or SOR.

Correlation analysis revealed K_i^{FD} to be significantly correlated with other parameters ($r = 0.99$, 0.86, 0.84 and 0.92 for K_i^{FD} correlations with K_i^{EFD}, K_i^P, K_i^{OCC} and SOR respectively; $p < 0.0001$ for all correlations, Fig. 3).

DISCUSSION

Our results suggest that because of its comparative superiority in discriminating mildly affected normals and in predicting clinical severity of disease, K_i^{FD} may be the optimum FDOPA/PET marker for the parkinsonian disease process. K_i^{EFD} may serve as a simple alternative to K_i^{FD} in circumstances in which HPLC analysis is unavailable. Although striatal K_i^P and K_i^{OCC} can discriminate PD patients from normals, these parameters were not as accurate as K_i^{FD}, and did not correlate as closely with independent disease severity measures. Our results indicate that the SOR, a simple semiquantitative index, can be used to discriminate mild PD from normal, but kinetic striatal K_i estimates appear to be necessary for quantitative correlations with disease severity measures.

K_i^{FD} is calculated based upon the time course of specific striatal radioactivity and the plasma FDOPA time-activity curve determined by arterial blood sampling and HPLC analysis. In order to correct the presence of radioactivity due to 3OMFD in the striatum, Martin et al. (*8*) determined

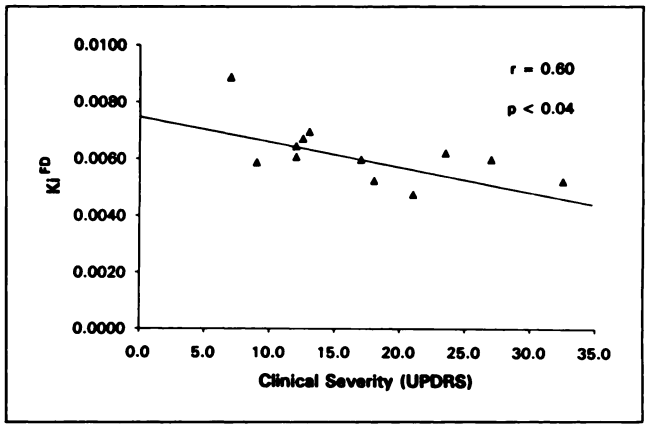

FIGURE 2. Correlation analysis of striatal rate constants for FDOPA uptake (K_i^{FD}) and motor disability [Unified Parkinson's Disease Rating Scale (UPDRS) composite motor scores; see text]. K_i^{FD} correlated significantly with overall motor disability scores ($r = -0.60$, $p < 0.04$).

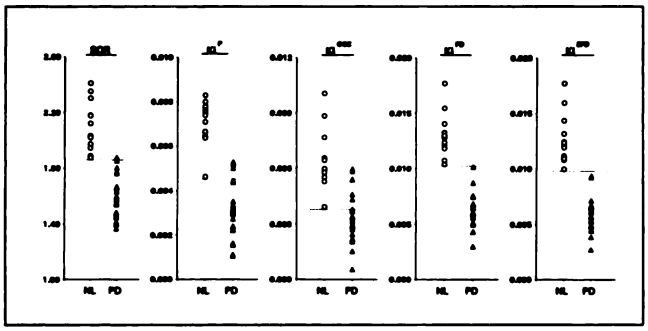

FIGURE 1. Comparison of the striato-to-occipital ratio (SOR) and striatal FDOPA uptake rate constants (K_i^P, K_i^{OCC}, K_i^{FD} and K_i^{EFD}; see text for definitions) measured in 12 normal volunteers (NL) and 12 patients with mild to moderate Parkinson's disease (PD). Mean values for all five parameters are significantly lower for the PD group as compared with normals ($p < 0.001$). K_i^{FD} values discriminated PD patients from normals most accurately, followed by K_i^{EFD}, K_i^P and SOR.

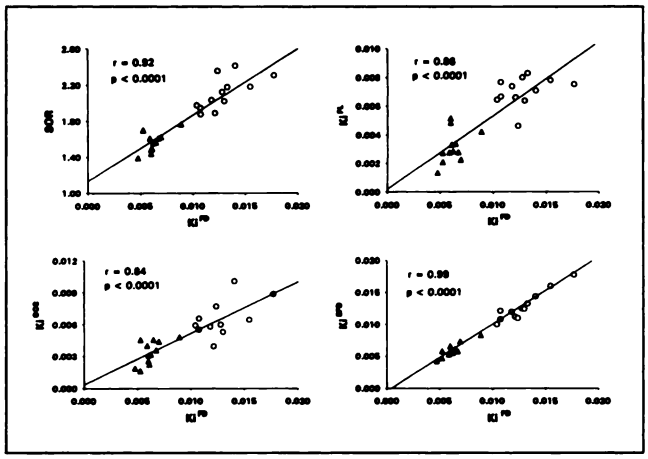

FIGURE 3. Correlations of striatal uptake rate constants for FDOPA (K_i^{FD}) with: (A) SOR; (B) K_i^P; (C) K_i^{OCC}, and (D) K_i^{EFD} in 12 normal subjects (○) and 12 PD patients (▲). Significant correlations ($r > 0.84$, $p < 0.0001$) were evident between K_i^{FD} and each of the other measured parameters.

specific striatal activity by subtracting occipital background radioactivity, reflecting nonspecific brain uptake of FDOPA and its metabolites, from total striatal radioactivity. This modification assumes that 3OMFD, which is formed peripherally and transported across the blood-brain barrier (BBB), is present in similar concentrations in the striatum and in the occipital region, and that there is negligible irreversible uptake of FDOPA or its metabolites in the occipital region. The former assumption has been supported by the experimental results using PET and 3OMFD as a tracer (*26–28*). The second assumption has also been validated previously (*8,13*). Therefore, although requiring HPLC analysis for calculation, K_i^{FD} takes into account the contribution of FDOPA metabolites in plasma and brain, and appears to be the most sensitive of the quantitative FDOPA/PET measures for the identification of early PD patients. This measure is also the best correlated with clinical disease severity.

Recently, it was suggested that K_i^{FD} does not reflect the striatal capacity for decarboxylation of FDOPA to ^{18}F-fluorodopamine when the large neutral amino acid (LNAA) transporter, which transfers FDOPA and 3OMFD across the BBB, is saturated (*29*). Because dietary LNAAs may nearly saturate the transporter at their normal plasma concentrations (*30*), these FDOPA/PET studies were performed after overnight fasting and withdrawal of levodopa for at least 12 hr. Under these conditions, plasma LNAA concentration has been shown not to reach the saturation level for the LNAA transport system (*9,31*). Additionally, administration of cold 3-OMD in clinically relevant concentrations failed to alter estimates of the blood-brain transfer rate constant (K_1) and the net decarboxylation rate constant (k_3) for FDOPA (*32*). Furthermore, if the transport system is variably saturated, K_i^{FD} and SOR may become uncorrelated. In this circumstance, K_i^{FD} may decrease (due to the reduction in K_1), while SOR remains unchanged (*31*). We found that K_i^{FD} is closely correlated with SOR (Fig. 3A). This suggests that in the fasting unmedicated state, K_1 variability is a small effect and does not interfere with the utility of K_i^{FD} as a clinically applicable parameter.

Use of the occipital input function in the MTGA obviates both arterial blood sampling and HPLC analysis. This completely noninvasive technique thus provides the most desirable alternative for the estimation of K_i value in the clinical setting (*12,13*). Nonetheless, the occipital time-activity curve is not a perfect substitute for the HPLC-corrected FDOPA time-activity curve because of the presence of 3OMFD in brain tissue. This is especially problematic with carbidopa pretreatment and rapid accumulation of 3OMFD in plasma (*33*). In the compartmental model for this method, the occipital lobe is regarded as a reference region which is assumed to fulfill the requirement that the contribution of radiolabeled metabolites to the measured radioactivity must be insignificant (*34*). This assumption is valid when L-[^{11}C]dopa is used as a tracer since L-[^{11}C]3-O-methyl-dopa has been shown to be formed slowly in the peripheral blood. However, FDOPA is metabolized much more rapidly to 3OMFD than L-[^{11}C]dopa to L-[^{11}C]3-O-methyl-dopa, especially following pretreatment with carbidopa (*33*). Thus, the contribution of 3OMFD to occipital time-activity curve may be larger in FDOPA/PET studies adding to the intersubject variability associated with these measurements. Conversely, blockade of the peripheral methylation of FDOPA using catechol O-methyltransferase (COMT) inhibitors may improve the accuracy of K_i^{OCC} measurements by simplifying the associated kinetic model (*16*). In addition, because of the larger intersubject variability in normals for K_i^{OCC} compared with K_i^{P} (which likewise neglects 3OMFD in the plasma and brain tissue), other factors, such as noise in the PET acquisition of the occipital time-activity curve, may contribute to the weaker discrimination and clinical correlation noted with K_i^{OCC}.

In agreement with our observations, previous investigations employing differing FDOPA/PET techniques have demonstrated that K_i^{FD}, K_i^{P} and SOR can each accurately differentiate PD patients from normals (*5,9–11,35*). However, in contrast to our findings, complete between-group separation has also been achieved with K_i^{OCC} (*11,12,29*). This discrepancy may be attributable to two factors.

First, in this investigation, we employed a whole striatal ROI including both caudate and putamen rather than separate ROIs for the small subregions. Because of signal-to-noise considerations and lack of availability of precise MRI coregistration, we opted for a larger composite striatal ROI. Theoretically, rate constants estimated for the putamen alone should provide better discrimination because of the preferential involvement of this region by the disease process (*12*). Nonetheless, in spite of this limitation, K_i^{FD} estimated for the whole striatum afforded excellent discrimination, suggesting that ROI subdivision may not be essential for between-group separation. Moreover, designation of putamenal boundaries may be quite difficult to achieve by visual inspection, especially in advanced patients with low putamenal FDOPA accumulation, and precise MRI-PET coregistration may be needed for this purpose. Nonetheless, noise levels may also increase in kinetic analysis of time-activity curves derived from such small regions even with co-planar MRI.

Second, because striatal K_i value falls with advancing disease (*5,9,10,12,13*), advanced PD patients may be easily differentiated using any of the uptake rate constants. For example, if we limited our discriminant analysis to the six more advanced patients (Hoehn and Yahr Stage III), striatal K_i^{OCC} achieved excellent between-group discrimination and misclassified only one parkinsonian striatum out of a possible 12. In all likelihood, our K_i^{OCC} measurements are less accurate as markers of early disease because of the specific technical issues associated with the acquisition of the occipital time-activity curve cited above.

Similarly, investigators have reported conflicting findings concerning the comparative clinical utility of these measures within subjects. Hoshi et al. (*29*) reported that

K_i^{OCC} could better differentiate PD patients from normal controls; K_i^{FD} was less sensitive than K_i^{OCC} as an index of nigrostriatal dysfunction. On the other hand, in experimental primate studies, Doudet et al. (*36*) noted that K_i^{FD} was superior by virtue of its closer correlation with independent dopaminergic parameters such as cerebro spinal fluid and homovanillic acid levels and motor performance. Our results support the latter findings.

We found that although K_i^{OCC} discriminated advanced patients with accuracy comparable to that of previous investigations (*29*), K_i^{FD} was a better discriminator of less severely involved patients. Indeed, K_i^{FD} values also predicted quantitative disease severity ratings with greater accuracy. Thus, our data support the use of K_i^{FD} as the optimal FDOPA/PET marker of the parkinsonian disease process. Nonetheless, K_i^{OCC} may be a useful noninvasive alternative to K_i^{FD}, especially in brain-dedicated PET systems where the occipital time-activity curve can be acquired with less noise, and perhaps with the adjunctive use of COMT inhibition (*37,38*). Indeed, the full comparative utility of these methods can be assessed only through an extensive study of PD patients, including those with minimal and preclinical involvement (*2*).

Although the actual metabolite-corrected plasma FDOPA time-activity curve appears to be the optimum input function for the calculation of K_i, this method requires extensive arterial blood sampling and HPLC analysis. However, this procedure adds to patient discomfort and is not without hazard to subjects and support personnel. Additionally, extensive blood sampling and processing is laborious, especially with HPLC analysis. As a less demanding clinically applicable alternative, we developed a simplified quantitative technique requiring only two arterial samples and no HPLC. By requiring only two arterial sticks, this method not only minimizes the number of blood samples for processing, but also eliminates the need for an indwelling arterial catheter. From a practical point of view, an arterial stick is substantially easier and safer, and involves less patient discomfort although both techniques require arterial puncture. A similar method has been developed by us for FDG/PET studies (*39*). Our method also obviates the need for HPLC analysis, making the use of FDOPA input function in MTGA more practical in the clinical research setting. Although not as fully noninvasive as the occipital input function method, this technique has the added advantage of not requiring head immobilization and sequential scanning for the entire 2-hr study period. In spite of the simplicity and ease of K_i^{EFD} estimation, this parameter agrees closely with K_i^{FD}, and in most respects is comparable as a marker of nigrostriatal dysfunction.

In summary, our data indicate that striatal K_i^{FD} measurement affords excellent discrimination of mild PD patients from age-matched normals, and correlates with independent disease severity measures. Other FDOPA/PET measures are generally less accurate as markers of the parkinsonian disease process. We found that K_i^{EFD}, estimated using a population-derived FDOPA input function with a standardized metabolite correction, provided an acceptable alternative to K_i^{FD} without requiring extensive blood sampling and HPLC. In all likelihood, the optimal choice of the input function for quantitative FDOPA/PET should be determined by the specific goals of the research study and technical resources available. For example, for a large study of preclinical cohorts, SOR may be advantageous by virtue of its simplicity and superior discrimination capability. In a longitudinal study of disease progression, such as assessing the effects of a neuroprotective agent or surgical intervention, K_i^{FD} may be optimal. In situations where brain-dedicated PET systems are available, K_i^{OCC} may be a simple noninvasive alternative. In most other circumstances, especially where HPLC analysis is not routinely performed, K_i^{EFD} may be an appropriate clinically useful choice.

APPENDIX

We developed a simplified technique to estimate a plasma FDOPA time-activity curve using two discrete arterial blood samples and two population-based curves: (1) A population-based plasma ^{18}F time-activity curve; and (2) a population-based FDOPA breakdown curve. Both population-based curves were generated based on the data obtained from 10 subjects (5 normal volunteers and 5 PD patients, 6 men and 4 women, mean age 49 ± 17 yr, range 23–76 yr) not included in the study population in this investigation. This technique consists of the following two steps.

Step 1: Estimating the Plasma ^{18}F Time-Activity Curve

This first step is an application of a simplified technique to estimate the plasma ^{18}F time-activity curve by scaling a population-based ^{18}F time-activity curve with two blood samples. We originally developed this method (*39*) to estimate the ^{18}F-fluorodeoxyglucose (FDG) input function for use in the autoradiographic equation (*40*).

A population-based plasma ^{18}F time-activity curve was generated by averaging the actual plasma ^{18}F time-activity curves from the 10 subjects described above. Prior to averaging, the time scale of each blood curve was corrected for the transit time from injection point to the sampling site (blood delay), and its amplitude was normalized by the mean activity of the two samples at the scaling time points (see below). At each time point (for the population time-activity curve), activities of individual blood curves were determined using linear interpolation if necessary, and then averaged to obtain the final activities for the population curve.

The timing of the optimal pair of blood samples for scaling the population-based time-activity curve was determined by examining the relationship between the ^{18}F activities of various timed blood samples and striatal K_i values. In each of 34 subjects (10 described above and 24 described in the text), we calculated a theoretical striatal K_i for FDOPA determined only by the plasma ^{18}F time-activity curve. This was done by the MTGA using individual plasma ^{18}F time-activity curves in conjunction with a standard FDOPA breakdown curve and a single, common striatal FDOPA time-activity curve taken arbitrarily from one of the studies. We correlated these theoretical K_i values with the mean activities in various plasma sample pairs to identify the paired samples which best predicted the K_i values. Because a hyperbolic relationship was found between the theoretical K_i values and mean activity of the plasma sample pairs, we calculated the cor-

TABLE A1
Correlation Coefficients of Reciprocals of Plasma Activities at Various Times with Theoretical K_i Values*

	A_5	A_{10}	A_{25}	A_{40}	A_{55}	A_{70}	A_{85}	A_{100}
A_5	0.970	0.985	0.990	0.988	0.987	0.986	0.985	0.984
A_{10}		0.992	0.996	0.997	0.995	0.994	0.992	0.991
A_{25}			0.992	0.991	0.989	0.986	0.984	0.982
A_{40}				0.988	0.986	0.982	0.979	0.976
A_{55}					0.982	0.977	0.972	0.967
A_{70}						0.970	0.964	0.957
A_{85}							0.954	0.945
A_{100}								0.934

*A_i-A_j represents the correlation coefficient between the theoretical K_i values and reciprocals of the mean activities for two samples taken at i and j min postinjection in 24 subjects. For instance, A_{10}-A_{10} represents the correlation coefficient between the K_i values and reciprocals of the activity of 10-min samples; A_{10}-A_{40} (underlined) represents the correlation coefficient between the K_i values and reciprocals of the mean activities for 10- and 45-min samples. Of the sample pairs examined, this pair provided the best correlation with theoretical K_i.

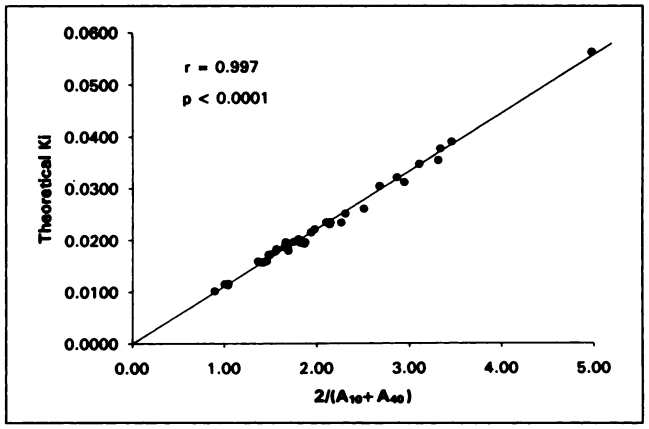

FIGURE A1. Correlation between the reciprocals of the mean ^{18}F activity of 10- and 40-min samples (A_{10} and A_{40}, respectively) and the theoretical K_i values calculated by the MTGA using individual plasma ^{18}F time-activity curves in conjunction with a standard FDOPA breakdown curve and a common striatal FDOPA time-activity curve.

relation coefficients between the reciprocals of the mean activity of various pairs and the theoretical K_i values (Table A1). The best correlation coefficient was provided by the mean activity of 10- and 40-min plasma samples (r = 0.997, Fig. A1), suggesting that these two samples may be the optimum pair to scale the population-based ^{18}F time-activity curve. Therefore, the plasma activities measured at these two time points were selected to obtain the individual scaling factor for the population-derived curve.

The estimated ^{18}F time-activity curve, $C_e(t)$, was obtained by scaling the population ^{18}F time-activity curve, $C_p(t)$, as follows:

$$C_e(t) = C_p(t - \delta) \times \frac{\overline{A_{10}A_{40}}}{\overline{C_{10}C_{40}}},$$

where

$$\overline{A_{10}A_{40}} = \frac{A_{10} + A_{40}}{2},$$

$$\overline{C_{10}C_{40}} = \frac{C_p(10 - \delta) + C_p(40 - \delta)}{2},$$

where A_{10} and A_{40} are the ^{18}F activities of the 10- and 40-min samples, and δ is estimated blood delay (min) which was obtained by adding 17 sec (an average lag time between brain delay and blood delay in our standardized injection) to the actually measured brain delay.

Comparison between the time integrals (area-under-the-curve; AUC) of the actual and estimated ^{18}F time-activity curves in 24 subjects is presented in Table A2. Mean differences (%) at 45, 55, 65, 75, 85 and 95 min postinjection, the time points used in the MTGA, ranged from −0.5% to 1.1%. Linear regression analysis for the AUC demonstrated excellent agreement between the actual and estimated ^{18}F time-activity curves at all the six time points (mean correlation coefficient: 0.998). These results are comparable to those we reported in FDG/PET studies (*39*), suggesting that a plasma ^{18}F time-activity curve can be accurately estimated using this two-point scaling method.

Step 2: Estimating the Plasma FDOPA Time-Activity Curve

Since we have found a relatively small variation of peripheral FDOPA breakdown rate across the subjects (see Table 2 in text), we used a population-based FDOPA breakdown curve to obtain an estimated plasma FDOPA time-activity curve from an estimated plasma ^{18}F time-activity curve without an individual HPLC analysis.

A population-based FDOPA breakdown curve was generated by averaging the actual FDOPA fractions from the 10 subjects at 10, 25, 40, 55, 70 and 85 min postinjection, and then fitting these six points plus an initial point (t = 0, fraction = 1) by the sum of two exponential decay functions (FDOPA/$^{18}F(t) = 0.41e^{-0.0079t} + 0.59e^{-0.054t}$, Fig. A2). Then, this function was applied to the estimated ^{18}F time-activity curve for the FDOPA metabolite correction to obtain the estimated FDOPA time-activity curve in the 24 subjects in the text.

The estimated FDOPA time-activity curve derived in this way was then used as an input function in an MTGA to calculate

TABLE A2
Comparison Between the Time Integrals of the Actual and Estimated Plasma ^{18}F Time-Activity Curves

	45 min	55 min	65 min	75 min	85 min	95 min
Mean differences (%)*	−0.2 ± 3.4	0.1 ± 2.9	0.4 ± 2.6	0.6 ± 2.5	0.9 ± 2.5	1.1 ± 2.6
Correlation coefficient	r = 0.998	r = 0.998	r = 0.998	r = 0.998	r = 0.998	r = 0.998

*Differences are expressed as [(estimate − actual)/actual] × 100 (%).

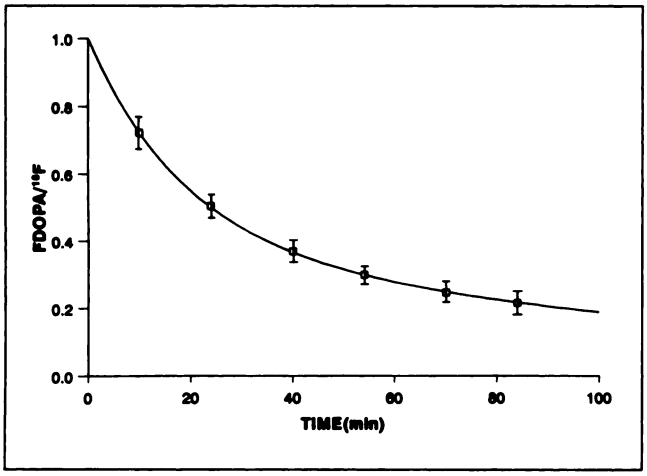

FIGURE A2. A population FDOPA breakdown curve generated by averaging the actual FDOPA fractions from 10 subjects at all six time points and fitting these six points plus an initial point (t = 0, fraction = 1) to the sum of two exponential decay functions (FDOPA/^{18}F = $0.41e^{-0.0079t} + 0.59e^{-0.054t}$).

striatal K_i measures (K_i^{EFD}; see text). A two-tailed paired-sample Student's t-test showed no significant differences between K_i^{FD} and K_i^{EFD} in 24 subjects ($p = 0.2$). Linear regression analysis for K_i^{FD} and K_i^{EFD} demonstrated excellent agreement ($r = 0.99$, $p < 0.0001$, $K_i^{EFD} = 1.02\,K_i^{FD} - 0.0004$; see Fig. 3D in text). Statistical analysis using a Student's t-test showed that the slope and y-intercept of this regression line is not significantly different from 1 and 0, respectively. The correlation coefficient between K_i^{FD} and K_i^{EFD} in the 12 PD patients ($r = 0.91$) was not significantly different from that calculated in the 12 normals ($r = 0.95$) as examined by a z-test ($p > 0.5$). This suggests that this technique is valid in both PD and normal populations. These results validate this simplified method for estimating a plasma FDOPA input function for an MTGA in FDOPA/PET studies. Because of the similarity of venous and arterial ^{18}F activity at times >15 min, this approach may also be implemented using venous samples for scaling.

ACKNOWLEDGMENTS

This work was supported by grants from the Parkinson Disease Foundation and the Dystonia Medical Research Foundation. Dr. Takikawa is a Veola T. Kerr fellow of the Parkinson Disease Foundation and Dr. Eidelberg is a faculty fellow of the Parkinson Disease Foundation and the United Parkinson Foundation. The authors thank Mr. Claude Margouleff and Ms. Janie Dill for help with the PET studies; Dr. Abdel Belakhlef and Mr. Ralph Mattachieri for cyclotron support; Dr. Debyendu Bandyopadyay for radiochemistry assistance; and Ms. Debra Segal for manuscript preparation.

REFERENCES

1. Brooks DJ. Detection of preclinical Parkinson's disease with PET. *Neurology* 1991;41(Suppl 2):24–27.
2. Burn DJ, Mark MH, Playford ED, et al. Parkinson's disease in twins: studies with ^{18}F-dopa and positron emission tomography. *Neurology* 1992; 42:1894–1900.
3. Freed CR, Breeze RE, Rosenberg NL, et al. Survival of implanted fetal dopamine cells and neurologic improvement 12–46 mo after transplantation for PD. *N Eng J Med* 1992;327:1549–1555.
4. Garnett E, Nahmias C, Firnau G. Central dopaminergic pathways in hemiparkinsonism examined by positron emission tomography. *Can J Neurol Sci* 1984;11:174–179.
5. Leenders KL, Palmer AJ, Quinn N, et al. Brain dopamine metabolism in patients with Parkinson's disease measured with positron emission tomography. *J Neurol Neurosurg Psychiatry* 1986;49:853–860.
6. Patlak CS, Blasberg RG, Fenstermacher JD. Graphical evaluation of blood-to-brain transfer constants from multiple-time uptake data. *J Cereb Blood Flow Metab* 1983;3:1–7.
7. Patlak CS, Blasberg RG. Graphical evaluation of blood-to-brain transfer constants from multiple-time uptake data generalization. *J Cereb Blood Flow Metab* 1985;5:584–590.
8. Martin WRW, Palmer MR, Patlak CS, Calne DB. Nigrostriatal function in humans studied with positron emission tomography. *Ann Neurol* 1989;26: 535–542.
9. Eidelberg D, Moeller JR, Dhawan V, et al. The metabolic anatomy of Parkinson's disease: complementary ^{18}F-fluorodeoxyglucose and ^{18}F-fluorodopa positron emission tomography studies. *Mov Disord* 1990;5:203–213.
10. Leenders KL, Palmer A, Turton D, et al. DOPA uptake and dopamine receptor binding visualized in the human brain in vivo. In: Fahn S, Marsden CD, Calne D, Goldstein M, eds. *Recent developments in Parkinson's disease*. New York: Reven Press; 1986:103–113.
11. Leenders KL, Salmon EP, Tyrrell P, et al. The nigrostriatal dopaminergic system assessed in vivo by positron emission tomography in healthy volunteer subjects and patients with Parkinson's disease. *Arch Neurol* 1990; 47:1290–1298.
12. Brooks DJ, Ibanez V, Sawle GV, et al. Differing patterns of striatal ^{18}F-Dopa uptake in Parkinson's disease, multiple system atrophy and progressive supranuclear palsy. *Ann Neurol* 1990;28:547–555.
13. Brooks DJ, Salmon EP, Mathias CJ, et al. The relationship between locomotor disability, autonomic dysfunction, and the integrity of the striatal dopaminergic system in patients with multiple system atrophy, pure autonomic failure, and Parkinson's disease, studied with PET. *Brain* 1990;113: 1539–1552.
14. Sawle GV, Colebatch JG, Shah A, Brooks DJ, Marsden CD, Frackowiak SJ. Striatal function in normal aging: implications for Parkinson's disease. *Ann Neurol* 1990;28:799–804.
15. Eidelberg D, Takikawa S, Dhawan V, et al. Striatal ^{18}F-DOPA uptake: absence of an aging effect. *J Cereb Blood Flow Metab* 1993;13;881–888.
16. Patlak CS, Dhawan V, Takikawa S, et al. Estimation of striatal uptake rate constant of FDOPA using PET: methodological issues. *J Cereb Blood Flow Metab* 1993;13(suppl 1):282.
17. Hoehn MM, Yahr MD. Parkinsonism: onset, progression and mortality. *Neurology* 1967;17:21–25.
18. Fahn S, Elton RL, and the UPDRS Development Committee. Unified Parkinson disease rating scale. In: Fahn S, Marsden CD, Calne D, Goldstein M, eds. *Recent developments in Parkinson's disease*, vol. 2. Floral Park, New Jersey: Macmillan; 1987:293–304.
19. Robeson W, Dhawan V, Takikawa S, et al. Super PETT 3000 time-of-flight tomograph: optimization of factors affecting quantification. *IEEE Trans Nucl Sci* 1993;40:135–142.
20. Kearfott KJ, Rottenberg DA, Knowles RJR. A new headholder for PET, CT and NMR imaging. *J Comput Assist Tomogr* 1984;8:1217–1220.
21. Luxen A, Milton P, Bida GT, et al. Remote, semiautomated production of 6-[^{18}F]fluoro-L-Dopa for human studies with PET. *Appl Radiat Isot* 1990; 41:275–281.
22. Dhawan V, Jarden JO, Strother S, Rottenberg DA. Effect of blood curve smearing on the accuracy of parameter estimates obtained for ^{82}Rb/PET studies of blood-brain barrier permeability. *Phys Med Biol* 1987;33:61–74.
23. Spetsieris P, Dhawan V, Takikawa S, Margouleff D, Eidelberg D. A versatile graphics-image processing package for imaging cerebral function. *IEEE Comput Graph App* 1993;13:15–26.
24. Talairach J, Tournoux P. *Co-planar stereotaxic atlas of the human brain*. New York: Thieme Medical Publishers, Inc.; 1988.
25. Anderson TW. *An introduction to multivariate statistical analysis*. New York: John Wiley & Sons; 1984.
26. Firnau G, Sood S, Chirakal R, Nahmias C, Garnett S. Metabolites of 6-[^{18}F]fluoro-L-Dopa in human blood. *J Nucl Med* 1988;29:363–369.
27. Doudet DJ, McLellan CA, Carson R, et al. Distribution and kinetics of 3-O methyl-6-[^{18}F]fluoro-L-DOPA in the rhesus monkey brain. *J Cereb Blood Flow Metab* 1991;11:726–734.
28. Melega WP, Grafton ST, Huang SC, Satyamurthy N, Phelps ME, Barrio JR. L-6-[^{18}F]fluoro-DOPA metabolism in monkeys and human: biochemical parameters for the formation of tracer kinetic models with positron emission

tomography. Tomographic studies. *J Cereb Blood Flow Metab* 1991;11: 890–897.
29. Hoshi H, Kuwabara H, Léger G, Cumming P, Guttman M, Gjedde A. 6-[^{18}F]fluoro-L-Dopa metabolism in living human brain: a comparison of six analytical methods. *J Cereb Blood Flow Metab* 1993;13:57–69.
30. Smith QR, Momma S, Aoyagi M, Rapoport SI. Kinetics of neutral amino acid transport across the blood-brain barrier. *J Neurochem* 1987;49:1651–1658.
31. Leenders KL, Poewe WH, Palmer AJ, Brenton DP, Frackowiak SJ. Inhibition of L-[^{18}F]fluorodopa uptake into human brain by amino acid demonstrated by positron emission tomography. *Ann Neurol* 1986;20:258–262.
32. Guttman M, Léger G, Cedarbaum JM, et al. 3-O-methyldopa administration does not alter fluorodopa transport into the brain. *Ann Neurol* 1992;31:638–643.
33. Melega WP, Luxen A, Permutter MM, Nissenson CHK, Phelps ME, Barrio JR. Comparative in vivo metabolism of 6-[^{18}F]fluoro-L-DOPA and [^{3}H]L-DOPA in rats. *Biochem Pharmacol* 1990;39:1853–1860.
34. Hartvig P, Ågren H, Reibring L, et al. Brain kinetics of L-[β-^{11}C]DOPA in humans studied by positron emission tomography. *J Neural Transm* 1991; 86:25–41.
35. Martin WRW. Dopa metabolism. In: Frost JJ, Wagner HN Jr., eds. *Quantitative imaging: neuroreceptors, neurotransmitters and enzymes*. New York: Raven Press; 1990:167–177.
36. Doudet DJ, Aigner TG, McLellan CA, Cohen RM. Positron emission tomography with ^{18}F-DOPA: interpretation and biological correlates in nonhuman primates. *Psychiatry Res Neuroimag* 1993;45:153–168.
37. Sawle GV, Burn DJ, Lammertsma AA, et al. PET demonstrates enhanced uptake of fluorodopa after peripheral COMT inhibition. *J Cereb Blood Flow Metab* 1993;13(suppl 1):294.
38. Guttman M, Léger G, Reches A, et al. Administration of the new COMT inhibitor OR-611 increases striatal uptake of fluorodopa. *Mov Disord* 1993; 8:298–304.
39. Takikawa S, Dhawan V, Robeson W, et al. Noninvasive quantitative FDG/PET studies using an estimated input function derived from a population arterial blood curve. *Radiology* 1993;188:131–136.
40. Phelps ME, Huang SC, Hoffman EJ, Selin C, Sokoloff D, Kuhl DE. Tomographic measurement of local cerebral glucose metabolic rate in humans with (^{18}F)2-fluoro-2-deoxy-D-glucose. Validation of method. *Ann Neurol* 1979;6:371–388.